Published in final edited form as:

FASEB J. 2020 March ; 34(3): 4602–4618. doi:10.1096/fj.201902594RR.

Mitochondrial adaptations to exercise do not require Bcl2-mediated autophagy but occur with BNIP3/Parkin activation

Sarah E. Ehrlicher[1], **Harrison D. Stierwalt**[1], **Benjamin F. Miller**[2], **Sean A. Newsom**[1], **Matthew M. Robinson**[1]

[1]School of Biological and Population Health Sciences, College of Public Health and Human Sciences, Oregon State University, Corvallis, OR, USA

[2]Aging and Metabolism Research Program,Oklahoma Medical Research Foundation, Oklahoma City, OK, USA

Abstract

Understanding the mechanisms regulating mitochondrial respiratory function and adaptations to metabolic challenges, such as exercise and high dietary fat, is necessary to promote skeletal muscle health and attenuate metabolic disease. Autophagy is a constitutively active degradation pathway that promotes mitochondrial turnover and transiently increases postexercise. Recent evidence indicates Bcl2 mediates exercise-induced autophagy and skeletal muscle adaptions to training during high-fat diet. We determined if improvements in mitochondrial respiration due to exercise training required Bcl2-mediated autophagy using a transgenic mouse model of impaired inducible autophagy ($Bcl2^{AAA}$). Mitochondrial adaptations to a treadmill exercise training protocol, in either low-fat or high-fat diet fed mice, did not require Bcl2-mediated autophagy activation. Instead, training increased protein synthesis rates and basal autophagy in the $Bcl2^{AAA}$ mice, while acute exercise activated BNIP3 and Parkin autophagy. High-fat diet stimulated lipid-specific mitochondrial adaptations. These data demonstrate increases in basal mitochondrial turnover, not transient activation with exercise, mediate adaptations to exercise and high-fat diet.

Keywords

mitochondrial respiration; protein turnover; skeletal muscle

Correspondence Matthew M. Robinson, School of Biological and Population Health Sciences, College of Public Health and Human Sciences, Oregon State University, 118F Milam Hall, Corvallis OR 97331, USA. matthew.robinson@oregonstate.edu.

AUTHOR CONTRIBUTIONS

SEE, HDS, SAN, and MMR planned the study, performed animal procedures and data collection. SEE performed majority of experiments, analysis, figure development and wrote the paper. BFM developed isotopic tracer analysis. All authors contributed to data interpretation and manuscript editing. MMR assumes full responsibility for dataset.

SUPPORTING INFORMATION

Additional supporting information may be found online in the Supporting Information section.

CONFLICT OF INTEREST

The authors have no conflicts to declare.

1 | INTRODUCTION

Skeletal muscle has a large tissue mass and high abundance of mitochondria, the major site of fuel metabolism and energy production, and contributes to whole-body metabolism. The mitochondrial reticulum undergoes continual turnover to maintain quality of the protein network and preserve metabolic function.[1] Protein synthesis and degradation pathways facilitate the turnover of mitochondrial proteins. Declines in skeletal muscle protein turnover rates are observed in metabolic diseases[2–4] and with advancing age.[5,6] Many metabolic and age-associated pathological conditions are also associated with mitochondrial defects or dysfunction.[7,8] Endurance exercise training improves mitochondrial oxidative function and whole-body metabolic health, in part by increasing skeletal muscle mitochondrial abundance[9] mediated by increases in mitochondrial biogenesis.[10] Further understanding of mitochondrial protein turnover regulation could inform strategies to maintain skeletal muscle health and alleviate burdens of metabolic disease.

Autophagy is responsible for the removal of low-functioning mitochondria, termed mitophagy,[11] to maintain overall mitochondrial function.[12] Exercise training enhances skeletal muscle protein degradation through global autophagy.[13] In mice undergoing aerobic exercise training, the loss of critical autophagy proteins, beclin-1 (Atg6),[14] Atg7,[15] or the mitophagy protein, Parkin,[16] blunts positive mitochondrial adaptations. These findings suggest the activation of autophagy mediates exercise-induced skeletal muscle mitochondrial adaptations. However, given the constitutive nature of knockout models, it is not possible to distinguish exercise-induced autophagy from basal autophagy. Conversely, $Bcl2^{AAA}$ transgenic mice allow for the isolation of stimulus-induced autophagy because of an alanine-substitution at a deactivating phosphorylation site.[17] In response to starvation or exercise, Bcl2 phosphorylation induces beclin-1 activation to increase autophagosome formation, but Bcl2 phosphorylation is absent in $Bcl2^{AAA}$ mice and restricts autophagy activation.[17] Following aerobic exercise training, $Bcl2^{AAA}$ mice had impaired exercise capacity[17] indicating a direct requirement for autophagy activation with exercise on training adaptations. Yet, the requirement of exercise-induced autophagy for improvements in mitochondrial protein turnover and respiratory function is not known.

Strategies to increase skeletal muscle mitochondrial protein turnover have strong therapeutic potential to improve whole-body metabolic health, especially during a stressed metabolic state such as obesity or Type 2 Diabetes. For example, exercise training restored mitochondrial efficiency in obese adults.[18] Further, while on a high-fat diet to induce obesity, $Bcl2^{AAA}$ mice had blunted improvements in whole-body glucose tolerance after exercise training,[17] suggesting a critical role of autophagy in the beneficial exercise effects on metabolic function. Therefore, activation of autophagy is a potential mechanism of exercise to improve mitochondrial function during metabolic stress.

Our primary aim was to determine the requirement of exercise-induced autophagy for mitochondrial adaptations to aerobic exercise training. We used the $Bcl2^{AAA}$ mouse model with restricted Bcl2-mediated autophagy in an 8-week exercise training study. We hypothesized the autophagy deficiency would impair the exercise-induced improvements to

mitochondrial respiration and protein turnover. Our secondary aim was to determine if high-fat feeding impaired the exercise-induced mitochondrial adaptations in $Bcl2^{AAA}$ mice.

2 | METHODS

2.1 | Animals and diets

Wild-type C57BL/6J male mice and transgenic Bcl2tm.1.1SJK (#018430) male mice were purchased from Jackson Laboratories (Bar Harbor, ME, USA) and matched for age (8–14 weeks old). The mice were group housed two to five per cage in 12:12-hour light-dark cycle at 22°C with free access to food and water and allowed to acclimate for at least one week before beginning the 12-week study. After 4 weeks, mice began graded aerobic exercise training (described below) or remained sedentary. In week 12, mice were euthanized 36 hours after the last bout of exercise and after a 4-hour fast to avoid alteration of autophagy markers by acute exercise,[19] postprandial[20] or prolonged fasting signals.[21] Mice were anesthetized with sodium pentobarbital overdose through an intraperitoneal injection and cardiac punctures were performed to collect plasma samples. Tissues were extracted and dissected then snap frozen in liquid nitrogen. At the end of the 12 weeks, mice were 24–28 weeks of age. The animal study protocol was approved by the Animal Care and Use Committee at Oregon State University (#4788). Group numbers were n = 12–17/group.

Mice consumed either a low-fat diet (LFD; D12450J; Research Diets, New Brunswick, NJ, USA) or high-fat diet (HFD; D12492; Research Diets, New Brunswick, NJ, USA) ad libitum for 12 weeks to induce obesity. The percent kilocalories from total fat (from lard)/carbohydrate/protein was 10/70/20 for the LFD (3.85 kcal/gm) and 60/20/20 for the HFD (5.24 kcal/gm). The diets were matched for sucrose content.

2.2 | Exercise training and acute exercise

Exercise training was performed on a motorized treadmill to standardize the amount of exercise for each group to 50 minutes per day, 5 days per week. Mice in the exercise groups acclimated to the motorized treadmill (Panlab, Harvard Apparatus, Holliston, MA, USA) over 1 week with a low speed and duration. Then, exercise bouts progressed in intensity and duration to reach 17 m/min for 50 minutes at 10% incline. Mice were encouraged to continue running with an air puff or mild shock plate at the back of the treadmill.

A graded exercise test was performed after the acclimatization and at the end of the training period to assess exercise capacity of the mice. The belt speed started at 6 m/min and 0% incline for 5 minutes then increased by 3 m/min and 5% incline every 2 minutes until 18 m/min and 15% incline was reached. The speed increased by 1–2 m/min every minute until exhaustion. The mice were removed from the treadmill when they refused to run, despite sitting on the shock grid for up to 5 seconds, and the total time was recorded.

The acute exercise bout consisted of intervals on the treadmill that alternated between a low-speed interval and high-speed interval at approximately 70% estimated maximal exercise capacity, based on the graded exercise test results of the training groups. The exercise bout started with the low-speed interval of 6 m/min at 5% incline for 5 minutes then progressed to the high-speed interval of 12 m/min (HFD) or 15 m/min (LFD) at 5% incline for 15 minutes.

The intervals were repeated twice then ended with a 5-minute cool down at 6 m/min. The total duration of exercise was 65 minutes. An intraperitoneal injection of sodium pentobarbital was given at 20 minutes postexercise and tissue harvest started at 30 minutes postexercise.

2.3 | Glucose and insulin tolerance testing

Glucose tolerance tests (GTT) and insulin tolerance tests (ITT) were performed in unrestrained mice at baseline and repeated at 4 weeks and 12 weeks. Mice were fasted and placed in individual cages with free access to water for 6 hours prior to the GTT and 4 hours prior to the ITT as previously described.[22] Body weight was recorded after the fasting period to calculate injection volumes. Blood glucose concentrations were measured by a handheld glucometer (Alphatrak2, Zoetis, Parsippany, NJ, USA) from a tail vein. Blood samples were also collected into a microhematocrit capillary tube from the tail vein to measure plasma insulin concentrations (Insulin ELISA, Alpco, Salem, NH, USA) immediately before and 15 minutes into the GTT. For the GTT, glucose was provided with an intraperitoneal injection of 2 g/kg body wt of a 20% dextrose solution. Blood glucose concentrations were measured at 0, 5, 15, 30, 60, and 120 minutes to calculate an area under the curve (AUC) for the full 2 hours. For the ITT, insulin (Humulin R; Eli Lilly, Indianapolis, IN, USA) was provided with an intraperitoneal injection at 0.5 IU/kg body wt. Blood glucose was measured at 0, 15, 30, 60, and 120 minutes and fall from baseline (FFB) was calculated in the first 30 minutes.

2.4 | Whole-body metabolic assessment

Metabolic rate was assessed by indirect calorimetry using a continuous metabolic monitoring system (Promethion, Sable Systems Int., Las Vegas, NV, USA). Mice were singly housed in the metabolic cages immediately after an exercise bout and given ad libitum access to food and water for a 12-hour dark cycle to monitor whole-body metabolism after exercise. The mice remained in the cages with access to food for a full 24-hour light/dark cycle to measure metabolism in a rested condition. The food was removed and mice remained in cages for 24 hours to measure metabolism in the fasted state. Air was sampled periodically from each cage and passed through a gas analyzer to determine oxygen (O_2) and carbon dioxide (CO_2) content at a constant flow rate of 2000 mL/min. Energy expenditure and respiratory exchange ratio (RER) was calculated based on VO_2 consumption and VCO_2 production[23] as either 1-hour or 12-hour averages for each cage. Physical activity was continuously measured by a multidimensional beam break system and food intake and body weight were continuously measured by electronic scales. Body composition was measured by dual-energy x-ray absorptiometry (Lunar PIXImus2, GE Healthcare, Madison, WI, USA) to quantify fat and fat-free (lean) mass.

2.5 | Deuterium oxide labeling

In week 10, mice received an intraperitoneal injection of D_2O saline solution (~99%; Cambridge Isotope Laboratories, Tewksbury, MA, USA) at 30 μL/g body wt to raise body water enrichment to ~5% (assuming 60% water weight) followed by continuous consumption of D_2O enriched at 8% in the drinking water.[22] Plasma samples collected at the time of euthanasia were analyzed for D_2O enrichment to calculate precursor enrichment. Plasma was placed in the inner well of an o-ring screw on cap and placed inverted on a

heating block overnight at 80°C. Next, 2 μL of 10 M NaOH and 20 μL of acetone were added to all samples and 20 μL of 0%−20% D_2O standards and capped immediately. Samples were vortexed at low speed and kept overnight at room temperature. Samples were extracted with 200-μl hexane, and the organic layer was transferred through anhydrous Na_2SO_4 into GC vials and analyzed via EI mode on an Agilent 7890B gas chromatograph coupled to an Agilent 5977B mass spectrometer with a DB-17MS column.

Quadriceps muscle was fractionated by differential centrifugation to subcellular fractions enriched with myofibrillar (MYO), subsarcolemmal mitochondrial (SSM), and intermyofibrillar mitochondrial (IMFM) proteins based on previously published methods.[24,25] Muscle samples (~70–80 mg) were powdered in liquid nitrogen, diluted in 1:20 (wt/vol) in homogenization buffer A (100mM KCl, 50mM Tris base, 5mM $MgCl_2$-$6H_2O$, 1.8mM ATP, and 1mM EDTA, pH 7.2) plus protease/phosphatase inhibitors (P8340, Sigma-Aldrich, St. Louis, MO, USA) and then homogenized using custom glass-on-glass homogenizers with 0.3-mm spacing between mortar and pestle for 10 minutes at 150 rpm. Samples were centrifuged for 10 minutes at 1000 *g* and 4°C to collect the MYO proteins. The supernatant was transferred to a new tube and centrifuged for 30 minutes at 9000 *g* and 4°C to collect the loosely bound SSM fraction. The MYO pellet was transferred back to the glass homogenizers and homogenized in 1-ml high-salt buffer (0.6 mol/L KCl and 20 mmol/L pyrophosphate-Na_4 decahydrate) for 5 minutes at 150 rpm to liberate the tightly bound IMFM proteins. Samples were centrifuged for 10 minutes at 1000 *g* and 4°C to collect the MYO fraction. The supernatant was transferred to a new tube and centrifuged for 30 minutes at 14 000 *g* and 4°C to collect the IMFM fraction. Protein fractions were hydrolyzed to amino acids, derivatized, and analyzed via EI mode on an Agilent 7890B gas chromatograph coupled to an Agilent 5977B mass spectrometer.

RNA was isolated from quadriceps muscle (~20 mg) using a commercially available kit (RNeasy Tissue Kit, Qiagen, Hilden, Germany). RNA was derivatized and analyzed via EI mode on an Agilent 7890B gas chromatograph coupled to an Agilent 5977B mass spectrometer.

The newly synthesized fraction of muscle proteins or RNA was calculated from the enrichment of labeled alanine bound to muscle proteins or RNA divided by the precursor enrichment. The precursor enrichment was calculated from D_2O enrichment in plasma, which was adjusted using mass isotopomer distribution analysis calculations.[26] The fraction new was then divided by time and multiplied by 100 to obtain the fractional synthesis rate (FSR).

2.6 | Mitochondrial preparation and respiration

Mitochondria were isolated from freshly dissected quadriceps muscle using differential centrifugation as previously described.[27] Muscle (~100 mg) was incubated in buffer A containing protease (Subtilisin A, P5380, Sigma-Aldrich, St. Louis, MO, USA) for 7 minutes on ice then homogenized in glass-on-glass homogenizers with 0.3-mm spacing between mortar and pestle for 10 minutes at 150 rpm. Samples were centrifuged for 5 minutes at 750 *g* and 4°C to collect the myofibrillar proteins. The supernatant was centrifuged for 5 minutes at 10 000 *g* and 4°C to pellet the mitochondria. The supernatant

was discarded and the mitochondrial pellet was washed with buffer A and centrifuged 5 minutes at 9000 *g* and 4°C. The supernatant was discarded and the mitochondria were resuspended in 1:4.2 (wt/vol) buffer B (180 mM sucrose, 35 mM KH_2PO_4, 10 mM Mg-Acetate, 5 mM EDTA, pH = 7.5).

High-resolution respirometry was performed using Oxygraph-2k units (Oroboros Instruments, Innsbruck, Austria) with MiR05 respiration buffer (0.5 mM EGTA, 3 mM $MgCl_2$-$6H_2O$, 60 mM lactobionic acid, 20 mM taurine, 10 mM KH_2PO_4, 20 mM HEPES, 110 mM sucrose, and 1 g/L bovine serum albumin). Two separate protocols were performed to measure oxygen consumption and hydrogen peroxide (H_2O_2) emission (10 μM Amplex red, 5 U/ml superoxide dismutase, and 1 U/mL horseradish peroxidase) as previously described and with a few variations.[22] Each protocol was performed in duplicate chambers (A and B) on one machine and the rate of oxygen consumed (JO_2 pmol O_2/sec/mL) at each point was calculated as the average values from the two chambers. Protein concentration of the mitochondrial preparation was measured by Pierce BCA assay (Thermo Fisher Scientific, Waltham, MA, USA) to calculate JO_2 relative to protein content (pmol O_2/μg protein/sec).

The approach outlined here provides assessment of oxidative phosphorylation, leak, and uncoupled state respiration. We conducted two independent protocols using lipid substrate (octanoyl-carnitine and malate [OCM]) or nonlipid substrates (glutamate, malate and succinate [GMS]) to determine rates of oxygen consumption (JO2). We measured leak respiration after the oxidative phosphorylation state with the addition of the complex V inhibitor, oligomycin, as an indicator of proton leak across the membrane. We then measured the contribution of electron transfer system (ETS) function to respiration by the addition of the membrane uncoupler, FCCP. The complex I inhibitor, rotenone was added to measure the contribution of S-linked substrates to ETS function. Full data sets from the two protocols in order of substrate addition are depicted in Supplemental Figure S4.

2.7 | Immunoblotting

Quadriceps and gastrocnemius muscle were homogenized as whole tissue (~40 mg) or mitochondrial isolations (~70 mg) for immunoblotting as previously described.[22] We previously reported, using proteomics, that the isolation yields a mitochondrial enriched fraction, but still has contamination of other fractions.[28] Immunoblotting of the Myo, Cyto and Mito fractions demonstrate a high abundance of VDAC in the Mito fraction with some contamination of tubulin (Figure 2D). Approximately 35 μg of protein was resolved on 10% −15% Bis-Tris gels and transferred to nitrocellulose membranes. A control sample was loaded at the beginning and end of each gel to serve as an internal control and their average intensity was used to normalize band intensities between gels. Ponceau staining of membranes was performed to verify equal loading and transfer of protein to the nitrocellulose membrane. Representative Ponceau images are provided in Figures S5-S8 with full representative blots for each data figure. For blotting of mitochondrial isolations, target antibodies were normalized to voltage dependent anion channel (VDAC, Abcam cat#14734) to account for variations in mitochondrial isolation in each sample. Membranes were blocked in 5% bovine serum albumin (BSA) in Tris-buffered saline + 1%Tween

(TBST). Primary antibodies were diluted in 5% BSA-TBST or 5% nonfat dry milk-TBST and membranes incubated overnight at 4°C. Primary antibodies OXPHOS cocktail (cat#110413), ETFA (cat#110316) and ETFB (cat#240593) were purchased from Abcam (Cambridge, UK). Primary antibodies LC3 (cat#12741), p62 (cat#39749), Parkin (cat#4211), BNIP3 (cat#3769), and Beclin-1 (cat#3495) were purchased from Cell Signaling Technology (Danvers, MA, USA). Primary antibody for HADH (cat#PA5–28203) was purchased from Thermo Fisher Scientific (Waltham, MA, USA). Secondary antibodies were purchased from Licor (Lincoln, NE, USA), diluted in 5% BSA-TBST or 5% nonfat dry milk-TBST and membranes incubated at room temperature for 1 hour. Images were generated using infrared detection (Odyssey, Licor, Lincoln, NE, USA) and analyzed using ImageView software (Licor, Lincoln, NE, USA).

2.8 | Statistical analysis

Comparisons between groups were performed using Student's *t* test or two-way analysis of variance model (ANOVA) by diet and exercise, as specified. Energy expenditure was analyzed by analysis of covariance (ANCOVA) with lean mass as a correlative variable. Statistical significance was set as $P < .05$. Statistical analysis was performed using Prism version 6 (GraphPad Software, La Jolla, CA, USA). Data are expressed as means with SD and group sizes are reported in figure legends.

3 | RESULTS

3.1 | Bcl2-mediated autophagy is not required for mitochondrial respiratory adaptations to exercise training

Our primary aim was to determine the requirement of inducible autophagy for mitochondrial adaptations in response to exercise training. Chronic knockout of autophagy proteins (ie, Atg7) leads to mitochondrial abnormalities.[29,30] Therefore, we used a mouse model that maintains basal rates of autophagy but cannot induce Bcl2-mediated autophagy in response to exercise.[17] This transgenic mouse model allows assessment of long-term requirement of inducible autophagy that is well suited for a training study. Twelve-week-old wild-type C57BL/6J (WT n = 13–17/group) and transgenic mice ($Bcl2^{AAA}$ n = 14–16/group) consumed a low-fat diet (LFD, 10% kcals from fat) and performed 8 weeks of exercise training or remained sedentary (EX and SED, respectively). The $Bcl2^{AAA}$ mice had usual basal phenotypic characteristics similar to WT. $Bcl2^{AAA}$ mice had similar body weights (SED, 28.5 ± 2.4 g; EX, 30.6 ± 3.6 g) compared with WT mice (SED, 29.1 ± 1.9 g; EX, 29.1 ± 2.4 g). Both genotypes increased time to exhaustion during a graded exercise test after the exercise training (WT, + 21%; $Bcl2^{AAA}$, + 33%; $P < .01$ pre vs post).

We used high-resolution respirometry on isolated mitochondria to test the requirement of inducible autophagy for improvements in respiratory function. Data are expressed as absolute values to indicate changes in respiration driven by total abundance, and also divided by mitochondrial protein concentration to indicate intrinsic functional changes. Contrary to expectations, $Bcl2^{AAA}$ mice had no impairments in complex I and II (CI + CII) substrate supported respiration after exercise training. Similar to WT, absolute rates of oxidative phosphorylation were higher after EX compared to SED in the $Bcl2^{AAA}$ mice (Figure 1A,

left axis). The relative rates of oxidative phosphorylation were not different between EX and SED groups in either WT or Bcl2^{AAA} mice (Figure 1A, right axis), suggesting changes in mitochondrial content drove improvements in oxidative phosphorylation capacity after exercise training. In both WT and Bcl2^{AAA} mice, the relative rates of proton leak were lower in the EX group compared to SED (Figure 1B), suggesting greater coupling of oxygen consumption to ATP-generation during oxidative phosphorylation. The ratio of oxidative phosphorylation to leak (respiratory control ratio; *P*/*L*) was 12% higher in the WT EX group compared with SED (t test, $P = .053$) further demonstrating that exercise increased coupling efficiency to improve oxidative phosphorylation. However, the respiratory control ratio was not significantly different in the Bcl2^{AAA} EX group compared with SED (*t* test, $P = .35$), indicating inducible autophagy promotes efficiency of mitochondrial respiration. The EX groups, regardless of genotype, had no difference in relative rates of CI + CII supported uncoupled respiration (Figure 1C, left) but slightly lower CII supported uncoupled respiration (Figure 1C, right) compared with SED. These data demonstrate that higher ATP-generating capacity, rather than electron transfer system (ETS) capacity, drove the higher CI + CII supported oxidative phosphorylation capacity with exercise training in both genotypes. Overall, mitochondrial respiratory adaptations to aerobic exercise training did not require exercise-induced autophagy through Bcl2. We next sought to identify the underlying mechanisms contributing to the intact mitochondrial respiration in the Bcl2^{AAA} mice.

3.2 | Greater protein turnover contributes to mitochondrial adaptations in autophagy-deficient mice

We determined if greater protein turnover could explain the maintained mitochondrial respiratory capacity in response to exercise training in the Bcl2^{AAA} mice. First, we measured markers of basal autophagy and mitophagy in skeletal muscle from the mice 36 hours after the last exercise bout and after a 4-hour fasting period. The autophagy marker microtubule-associated protein 1A/1B light chain 3A (LC3) is converted from LC3-I to LC3-II upon activation of autophagosome formation, therefore both the total abundance of LC3 and the ratio of LC3II/LC3I indicate autophagosome abundance.[31] In WT mice, the EX group had higher LC3I content and LC3II content but no difference in the ratio of the LC3II/I compared with SED (Figure 2A). In contrast, the Bcl2^{AAA} EX group had a higher ratio of LC3 II/I driven by greater LC3II content compared with SED (Figure 2A), suggesting greater basal autophagy. Additionally, Bcl2^{AAA} mice had greater mitochondrial LC3II content compared with WT (Figure 2E), suggesting greater basal mitophagy. The autophagy receptor p62 is downstream of formation and degraded with the autophagosome to indicate autophagosome clearance.[31] The effect of exercise training on p62 was also different between the genotypes, where the EX group had higher p62 content in WT but lower content in the Bcl2^{AAA} mice (Figure 2B). The Bcl2^{AAA} SED group had a higher protein content of p62 compared with WT SED (Figure 2B), suggesting restricted autophagosomes clearance in the Bcl2^{AAA} SED mice that was improved in the EX group. Additionally, the EX groups of both WT and Bcl2^{AAA} mice had lower mitochondrial p62 content compared with SED (Figure 2F). Beclin-1 forms a kinase complex involved in autophagosome formation and is bound to Bcl2 to prevent induction of autophagy.[32] The Bcl2^{AAA} SED group had a higher protein content of Beclin-1 compared with WT SED (Figure 2C), suggesting a compensation in autophagosome formation potential in the

$Bcl2^{AAA}$ mice that was restricted in the EX group. Overall, these markers suggest that the exercise trained $Bcl2^{AAA}$ mice had higher basal autophagy and mitophagy compared with the sedentary mice, as a compensation for restricted exercise-induced autophagy.

We used deuterium oxide (D_2O) labeling for the final two weeks of the exercise training to measure protein and RNA synthesis rates including two mitochondrial fractions isolated from skeletal muscle. In the $Bcl2^{AAA}$ mice, the EX group had greater subsarcolemmal mitochondria (SSM) protein synthesis compared with SED (Figure 2H, left), an effect not observed in WT. There were no differences between EX and SED groups in intermyofibrillar mitochondria (IMFM) protein synthesis rates (Figure 2H, right), indicating a fraction specific effect of exercise-induced mitochondrial biogenesis. There were no differences between groups in myofibrillar (MYO) protein synthesis rates (Figure 2I) or RNA synthesis (Figure 2J), indicating a lack of difference in global protein synthesis and ribosomal biogenesis. These data demonstrate that exercise training increased mitochondrial biogenesis in the $Bcl2^{AAA}$ mice, matching the increase in basal autophagy to promote mitochondrial protein turnover.

We next considered if changes in protein abundance of the mitochondrial respiratory chain complexes accompanied the greater respiratory capacity. The $Bcl2^{AAA}$ EX group had consistently greater protein abundance of representative subunits of respiratory complexes I-V compared with SED (Figure 2K), while WT EX mice had greater abundance of complex IV only compared with SED (Figure 2K). The accumulation of mitochondrial proteins in the $Bcl2^{AAA}$ mice may be due to a combination of suppressed mitochondrial protein degradation after exercise and higher protein synthesis rates.

Thus far, our data demonstrate that restricting exercise-induced autophagy through the Bcl2 pathway did not impair mitochondrial respiratory adaptations to exercise training, likely because of compensatory increases in basal autophagy and mitochondrial protein synthesis. Additional stress on protein turnover may reveal a more significant role of exercise-induced autophagy through the Bcl2 pathway for maintaining mitochondrial respiratory function. High-fat feeding is a model that increases reliance on whole body and mitochondrial lipid respiration, which we and others have shown increases mitochondrial abundance and protein turnover[22,33] and possibly restricts adaptations to exercise.[34] Compensatory changes in protein turnover may occur differently during high-fat feeding, when autophagy may be compromised. Therefore, we next examined whether mitochondrial respiratory adaptations to exercise training require exercise-induced autophagy during the metabolic stress of high-fat feeding.

3.3 | Whole-body metabolic phenotype following high-fat feeding and exercise training

We used high-fat feeding as a metabolic challenge to induce changes in whole-body and mitochondrial respiration. C57BL/6J WT and $Bcl2^{AAA}$ mice consumed a high-fat diet (HFD, 60% kcal from fat) for 4 weeks followed by 8 weeks of exercise training or sedentary behavior (EX and SED, respectively) (Figure 3A). During week 10, mice were individually housed in metabolic cages for 3 days to measure whole-body metabolism.

The whole-body phenotype due to HFD in both WT and $Bcl2^{AAA}$ mice was, as expected, weight gain (Figure 3B,C), hyperglycemia (Figure 3D) and hyperinsulinemia (Figure 3E), with minor improvements in the EX groups. Glucose and insulin tolerance were impaired in the $Bcl2^{AAA}$ mice compared with SED, but exercise training improved glucose and insulin tolerance in both genotypes (Figure 3F,G). Time to exhaustion improved after exercise training in both genotypes during HFD (WT, + 27%; $Bcl2^{AAA}$ + 21%; $P < .01$ pre vs post). Daily exercise bouts of 400–800 m more than doubled the normal daily in-cage distance covered for the EX groups (Figure S2A). Food intake measured during week 10 indicated lower consumption of HFD in grams that resulted in similar kcal intake to LFD in SED mice. The exercised mice had no apparent compensation in food intake (Figure S2B).

Whole-body respiratory exchange ratio (RER) indicated chronic reliance on lipid oxidation among HFD mice, which was similar between SED and EX groups (Figure 3H upper panel). Absolute energy expenditure rates (EE kcal/hour) were similar across genotype and exercise groups (Figure 3H lower panel). Among SED groups, mice eating HFD had proportionally greater increases in EE per lean mass (Figure S2C), which was restored by exercise training (Figure S2D).

3.4 | High-fat feeding did not impair mitochondrial adaptations to exercise training

We determined the requirement of inducible autophagy for improvements in mitochondrial respiration after exercise training during the added metabolic stress of high-fat feeding. We measured respiratory rates in isolated mitochondria as described above (Figure 1). Regardless of genotype, the EX groups had higher absolute rates of oxidative phosphorylation compared with SED but had lower rates relative to protein content compared with SED (Figure 4A). High-fat feeding did not impair the exercise-induced increase in mitochondrial protein abundance but may have compromised complex I and complex II substrate supported respiratory function.

We determined if high-fat feeding compromised protein turnover in a way that would alter the exercise training effects on CI + CII supported respiratory capacity. HFD did not impair mitochondrial protein synthesis rates in the $Bcl2^{AAA}$ mice (Figure 4B). In fact, the effect of exercise was close to significant ($P = .07$) for higher SSM protein synthesis. $Bcl2^{AAA}$ mice had higher mitochondrial LC3II content compared with WT mice. The EX groups, regardless of genotype, had higher mitochondrial LC3II content compared with SED (Figure 4C). Basal autophagy markers, LC3 I and p62, were higher in the HFD $Bcl2^{AAA}$ mice, in both the SED and EX condition, compared with WT (Figure 4F,G), possibly as an indication of suppressed global autophagy. However, the EX groups, regardless of genotype, had higher LC3II content (Figure 4F) while the EX $Bcl2^{AAA}$ mice had a greater ratio of LC3II/I content (Figure 4F). Together these data suggest HFD did not impair exercise-induced basal autophagy or mitophagy in the $Bcl2^{AAA}$ mice.

Contrary to expectations, high-fat feeding did not impair exercise adaptations in the $Bcl2^{AAA}$ mice. Our data suggest 12 weeks of high-fat feeding did not compromise skeletal muscle protein turnover or prevent adaptations to exercise-training. Due to the large dietary lipid availability for the HFD mice, we next wanted to determine if exercise training impacted mitochondrial respiration of lipid substrates differently than nonlipid substrates.

3.5 | Independent effects of exercise and high-fat feeding to induce mitochondrial lipid oxidation adaptations

We examined mitochondrial lipid respiratory changes in response to high-fat feeding and exercise training by using high-resolution respirometry on isolated mitochondria. In both WT and $Bcl2^{AAA}$ mice, EX had a main effect to increase absolute rates of lipid-supported oxidative phosphorylation compared with SED, but not relative to protein content (Figure 5A,D). Independent of EX, the HFD groups had greater lipid oxidation in both absolute units and relative to protein content compared with the LFD groups (Figure 5A,D), suggesting the improvements in oxidative phosphorylation capacity with HFD were due to intrinsic remodeling of the mitochondria more so than increased total protein abundance.

In WT mice, greater electron transfer system capacity (Figure 5C), rather than greater proton leak (Figure 5B), contributed to the HFD-induced increase in lipid oxidation compared with LFD. In fact, the respiratory control ratio (*P*/*L*) was greater in the HFD SED (+59%, $P < .001$) and HFD EX (+57%, $P < .001$) groups compared to the respective LFD groups, demonstrating increased coupling efficiency of lipid oxidation following HFD. The electron leak to H_2O_2 was higher for lipid-substrates than nonlipid substrates in WT mice (Figure 5G), which agrees with lipid-induced production of reactive oxygen species.[35] There were significant main effects for both diet and exercise to lower electron leak for only lipid substrates, suggesting improved lipid oxidation efficiency following either HFD or EX. Interestingly, the $Bcl2^{AAA}$ mice were more susceptible to HFD-induced leak respiration (Figure 5E) and had a blunted main effect of EX to improve electron leak to H_2O_2 (Figure 5H). Though, the respiratory control ratio (*P*/*L*) was still much greater in the HFD SED (+49%, $P < .001$) and HFD EX (+60%, $P < .001$) groups compared to the respective LFD groups.

We considered if changes in lipid oxidation protein abundance accompanied the greater lipid respiratory capacity. In both genotypes, EX and HFD had main effects to increase content of electron transfer flavoprotein (ETF) α/β subunits, while HFD groups additionally had greater hydroxyacyl-coenzyme A dehydrogenase (HADH) content (Figure 5I,J). The increase in ETF and HADH coincide with greater respiratory chain complexes and increased mitochondrial respiratory capacity.

The lipid respiration data further demonstrate mitochondrial adaptations did not require Bcl2-mediated autophagy activation, though there was a loss in mitochondrial efficiency with high-fat feeding in $Bcl2^{AAA}$ mice that did not occur in the WT mice. The lipid respiration results indicated a strong remodeling of the mitochondria to increase lipid respiratory capacity and protein abundance in response to exercise and high-fat feeding that did not require Bcl2-mediated autophagy.

3.6 | Exercise training and acute exercise upregulates parallel autophagy pathways during high-fat feeding

The findings in the current study suggest parallel autophagy pathways to Bcl2 are sufficient to mediate mitochondrial remodeling during exercise training. Therefore, we next measured the effect of exercise training on markers of Bcl2-independent mechanisms of mitophagy.

Alternative pathways include ubiquitin-mediated targeting of membrane proteins or autophagy receptors residing on the outer mitochondrial membrane. Parkin, an E3 ligase, tags mitochondria for degradation through the mitophagy pathway[36] and Bcl-2/adenovirus E1B interacting protein 3 (BNIP3) is a mitophagy receptor that resides on the outer mitochondrial membrane.[37] Total Parkin and BNIP3 abundance were not different between SED and EX in either WT or $Bcl2^{AAA}$ mice (Figure S3A,B). In the WT mice, mitochondrial Parkin (Figure 6A) and BNIP3 content (Figure 6B) was largely unchanged, except for elevated BNIP3 content in the HFD EX group compared with HFD SED. In the $Bcl2^{AAA}$ mice, LFD EX mice had lower mitochondrial Parkin (Figure 6A) but higher BNIP3 content (Figure 6B) compared with LFD SED. The $Bcl2^{AAA}$ HFD mice also had lower mitochondrial Parkin content (Figure 6A) and higher BNIP3 content (Figure 6B) compared with LFD. Together, these data suggest BNIP3 may be a mediator of HFD and exercise-induced increases in basal mitophagy in both WT and $Bcl2^{AAA}$ mice. Since these markers were measured after exercise training and after mitochondrial adaptations have occurred, we did not capture the transient activation of mitophagy mediators with exercise.[38]

To consider the possibility that $Bcl2^{AAA}$ mice retain the ability to activate Bcl2-independent mechanisms of mitophagy in response to exercise, we added groups that performed an acute bout of exercise. These groups underwent 12 weeks of LFD or HFD, and then had tissues collected 30 minutes after a single bout of treadmill exercise (65 minutes at 12–15 m/min). Parkin localization to mitochondria was greater after acute exercise compared with SED in $Bcl2^{AAA}$ mice, a difference not observed in the WT mice (Figure 6D). The greater Parkin was not due to changes in total Parkin as there were no differences in total skeletal muscle Parkin abundance after a single bout of exercise (Figure 6E). Additionally, BNIP3 abundance was greater in the mitochondrial fraction after acute exercise compared with SED in both the WT and $Bcl2^{AAA}$ mice (Figure 6F). The acute exercise data indicated a compensatory activation of Parkin and BNIP3 with exercise that may mediate mitophagy despite impaired Bcl2-mediated inducible autophagy.

4 | DISCUSSION

We investigated the requirement of Bcl2-mediated autophagy for mitochondrial adaptations to aerobic exercise training to determine the specific requirement of exercise-induced autophagy on mitochondrial remodeling and respiratory function. There is a growing body of research that supports mitophagy contributes to beneficial mitochondrial adaptations to metabolic stress, such as exercise.[39,40] Current understanding is that activation of general autophagy signaling through ULK1 is required for induction of mitophagy by exercise.[37] Identifying additional regulators of mitophagy is important for understanding the overlap of the general autophagy and mitophagy pathways in response to exercise. Contrary to expectations, mitochondrial respiratory adaptations to exercise training did not require exercise-induced activation of autophagy through the Bcl2 pathway. Rather, our data revealed that $Bcl2^{AAA}$ mice had compensatory increases in basal autophagy and mitochondrial biogenesis with exercise training that occurred with increased mitochondrial Parkin localization and maintained BNIP3 abundance. Additionally, high-fat feeding did not impair the mitochondrial respiratory adaptations to exercise training in the $Bcl2^{AAA}$ mice. High-fat feeding induced significant increases to lipid-specific oxidation and intrinsic

mitochondrial remodeling, independent of exercise training. Overall, our findings support that the exercise training effects to improve mitochondrial respiratory capacity are through enhanced basal autophagy and Bcl2-independent pathways and support a model by which HFD drives mitochondrial respiratory adaptations, not overt dysfunction.

Mitophagy is a primary pathway for degrading damaged portions of the mitochondrial reticulum[29] that is constitutively active and inducible under stress conditions. In mice performing endurance exercise training, partial knockout of beclin-1 ($Atg6^{+/-}$), a critical autophagy protein, blunts the gain in mitochondrial content in skeletal muscle,[14] but this deletion does not distinguish between basal and inducible autophagy. Our results demonstrate that mitochondrial respiratory capacity increases after exercise training in transgenic mice with impaired inducible Bcl2/beclin-1 autophagy similar to the WT mice. We also observed greater basal content of the autophagy markers LC3, p62, and beclin-1 in the $Bcl2^{AAA}$ mice compared with WT, which was not observed in the $Atg6^{+/-}$ mice.[14] Additionally, we observed an increase in LC3 accumulation in the mitochondrial fraction in the $Bcl2^{AAA}$. Basal rates of autophagy and mitophagy may compensate in the $Bcl2^{AAA}$ mice to maintain mitochondrial degradation, suggesting the acute rise in autophagy after each exercise bout is not required for mitochondrial adaptations to exercise training.

Exercise-regulated autophagy also appears to involve mitochondrial autophagy receptors to target specific portions of the mitochondrial reticulum for degradation.[19,38] Several studies have shown exercise increases the protein abundance of BNIP3, a mitochondrial autophagy receptor, in skeletal muscle.[13,14,41] Additionally, the E3 ligase, Parkin localizes to the mitochondria after acute exercise to recruit autophagosomes.[16] After exercise training, Parkin KO mice had greater skeletal muscle mitochondrial content but with impaired respiratory function.[16] In our study, acute exercise increased Parkin and BNIP3 accumulation in the mitochondrial fraction of skeletal muscle in $Bcl2^{AAA}$ mice similar to WT. These results are significant because they demonstrate that exercise activates mitochondrial autophagy independently of Bcl2-mediated autophagy and suggests the regulation of autophagy for mediating mitochondrial protein turnover occurs parallel to other exercise regulated autophagy pathways (eg, glucose adaptations). The autophagy pathways regulating mitochondrial adaptations appear distinct from those regulating substrate turnover, such as glucose. It is possible that more downstream proteins to Bcl2, such as Parkin/BNIP3, directly regulate mitophagy. Based on our findings and previously published studies, it appears constitutive autophagy[42] and inducible mitochondrial autophagy[16] maintain the mitochondrial reticulum independent of Bcl2, while Bcl2 is required for glucose adaptations.

Exercise stimulates mitochondrial protein synthesis as a critical mechanism of enhancing protein turnover for mediating mitochondrial adaptations.[43,44] Skeletal muscle mitochondria can be isolated in two different fractions, SSM and IMFM, which have distinct biochemical properties and responsiveness to exercise training.[45] We provide measurements of long-term fractional synthesis rates of these two mitochondrial populations. Exercise training stimulated SSM, but not IMFM, protein synthesis in the $Bcl2^{AAA}$ mice. The SSM fraction appears particularly responsive to aerobic training including changes to lipid metabolism in lean mice.[45] The enhanced mitochondrial biogenesis is likely a compensatory mechanism to

preserve mitochondrial function in $Bcl2^{AAA}$ mice. Our results are consistent with other studies that demonstrate increases in both mitochondrial biogenesis and autophagy as a mechanism of mitochondrial adaptations to exercise.[13,38] Such selective remodeling of mitochondria has been demonstrated in caloric restriction—a period of preservation of mitochondrial proteins[24,46]— that may regulate through mechanistic target of rapamycin complex 1, a potent nutrient sensor between both autophagy and translational machinery.[47]

High-fat feeding results in an overload of lipids that drives lipid oxidation without high energy demands, putting stress on mitochondrial metabolism.[48] High-fat feeding in mice with a skeletal muscle knockout of Atg7, an autophagy machinery protein, impaired mitochondrial function,[15] further supporting the role of autophagy in preserving mitochondrial function during metabolic stress. In our study, both WT and $Bcl2^{AAA}$ mice had improved mitochondrial lipid oxidation capacity after high-fat feeding, despite glucose intolerance. The addition of exercise training improved glucose tolerance in the WT mice and to a lesser extent in the $Bcl2^{AAA}$ mice, which was similar to the phenotype previously reported.[17] The increased mitochondrial respiration with HFD remained even after accounting for protein abundance, while the exercise training effects were due to increased protein abundance. Unlike WT mice, the HFD $Bcl2^{AAA}$ mice had a slightly but significantly higher leak respiration compared with LFD. Exercise training did not alter the lipid-supported leak respiration, nor did it lower the electron leak to H_2O_2, further demonstrating impaired mitochondrial efficiency in the HFD $Bcl2^{AAA}$ mice. These results are informative because they suggest maintaining mitochondrial function during high-fat feeding does not require Bcl2-mediated autophagy. However, declines in mitochondrial efficiency and energy wasting are potential protective mechanisms for preserving mitochondrial function in the autophagy deficient mice.[49,50] Further, exercise-induced mitochondrial adaptations do not rely more on Bcl2-mediated autophagy in a metabolically stressed state.

High-fat feeding (eg, 45%−60% fat) increases mitochondrial protein abundance and respiration in rodent models, especially lipid oxidation proteins.[33,51] The electron transfer flavoprotein (ETF) is the direct entry point for reducing equivalents from lipid oxidation into the electron transfer system.[52] Knockout of its upstream suppressor increased ETF activity and promoted lipid oxidation in response to high-fat excess,[53] though response to exercise training is less known. Our data demonstrate increased protein abundance of ETF alongside greater lipid supported oxidative phosphorylation after high-fat feeding and exercise training. The implications of our findings are that high-dietary fat and exercise training stimulate mitochondrial lipid oxidation capacity through common mechanisms of increased ETF.

We conclude that the mitochondrial adaptations to exercise did not depend on Bcl2-mediated autophagy in either LFD or HFD mice. Instead, exercise activated the mitochondrial-specific autophagy mediators, Parkin and BNIP3, as parallel mechanisms for mitochondrial clearance. Exercise activated basal autophagy and mitochondrial biogenesis to mediate mitochondrial adaptations. Further, HFD led to pronounced increases, not impairments, in mitochondrial respiration. Mitochondria had intrinsic remodeling, via enhanced protein synthesis and degradation, and greater lipid oxidation capacity as an adaptation to HFD with no evidence of impaired autophagy or exercise adaptations. Our data support that chronic

increases in basal rates of mitochondrial autophagy, not the transient exercise induction, and protein synthesis maintain mitochondrial respiratory function to meet demands of metabolic stress.

5 | LIMITATIONS AND CONSIDERATIONS OF THE STUDY

We acknowledge the limitations of using static measurements of autophagy protein markers as a surrogate for pathway flux. We interpret our measures of autophagosome abundance as potential for autophagy rather than completion of autophagy. To decrease technical variation, we incubated membranes in single antibody solutions and imaged together as batch analyses. We included positive controls (cell lysates treated with chloroquine, an autophagy inhibitor) to identify autophagy markers. Additionally, we used multiple markers to distinguish various stages of autophagy/mitophagy to gain a more comprehensive understanding of pathway changes. To increase confidence in static measures, we carefully considered the timing for measuring basal autophagosome abundance to avoid acute stimuli. Mice were euthanized 36 hours after the last bout of exercise based on previous literature demonstrating transient activation of autophagy with exercise that resolved within 24 hours.[19] Mice were also fasted for 4 hours before being euthanized to avoid suppression of autophagy by postprandial rises in insulin and glucose,[20] but also to avoid activation of autophagy that occurs within 12 hours of food deprivation.[21]

The timing of D_2O administration was the final two weeks, after 6 weeks of the exercise intervention. Therefore, the results must be interpreted in context of maintenance, not initial exercise training adaptations. Synthesis rates are an average of all proteins in the sample and vary between individual proteins.[54] Increases in pool size is also a consideration during the extended labeling periods.[55] Expansion of the mitochondrial reticulum during the 14-day labeling period would mean the absolute synthesis rates were higher than our measured fractional synthesis rates.

We used isolated mitochondria for respiration while other studies use permeabilized muscle fibers. We chose to use isolated mitochondria to avoid potential limitations on substrate trafficking and sample a larger portion of the mitochondrial reticulum from a larger starting tissue (~100 mg vs 2–3 mg for permeabilized fibers). An important consideration is that the permeabilized fiber method retains more of the intrinsic morphology of the mitochondrial reticulum during the respiration measurements.[56] The processes of mitochondrial membrane fusion and fission appear interdependent with mitophagy for the maintenance of overall mitochondrial health.[57] Previous reports using both isolated mitochondria and permeabilized fibers (in context of aging and caloric restriction) demonstrate similar qualitative results between both preparations.[46] We cannot exclude the possibility that the respiratory capacity of the intact mitochondrial reticulum is compromised in the $Bcl2^{AAA}$ mice after exercise training. We did not measure ATP production directly. The greater oxidative phosphorylation capacity—without changes in leak (oligomycin inhibited)—is consistent with greater capacity for ATP production following HFD or exercise training. Also, our respiratory protocol does not measure full TCA or glycolysis capacity in isolated mitochondria. Supercomplex assembly within the electron transfer system could be an underlying

mechanism of improved respiration independent of protein content.[58] Muscle fibers retain such in-vivo characteristics of oxidative pathways.

An important consideration is HFD mice gained weight throughout the study due to positive energy balance of the HFD. Therefore, the high-fat feeding model cannot differentiate between the effects of obesity and high lipid intake from the diet on mitochondrial adaptations. Next steps include distinguishing the negative influence of obesity independent from dietary lipid availability on bioenergetics.[59] Indeed, non-obese models of insulin resistance had limited differences in mitochondrial lipid respiration vs weight-matched controls.[60] Mitochondria have a robust capacity to adapt to changing bioenergetic stimuli ranging from obesity to caloric restriction.[46] Measurements taken after a longer diet intervention, to achieve weight-stable obesity, may alter metabolic and mitochondrial function than the current 12-week diet intervention.

The study included only male mice though it is of interest to study potential sex differences in mitochondrial respiratory adaptations. Intrinsic mitochondrial respiration in skeletal muscle is different between men and women.[61] Further, female mice are more susceptible to loss of mitochondrial quality in response to impaired autophagy.[42] It is necessary for future studies to investigate potential sex differences in the role of selective autophagy for mitochondrial adaptations to exercise and high-fat feeding.

Supplementary Material

Refer to Web version on PubMed Central for supplementary material.

ACKNOWLEDGMENTS

We thank Emily Burney and Bergen Sather (Oregon State University), Dr. Felix Morales-Palomo (University of Castilla-La Mancha, Spain) and Frederick Peelor (Oklahoma Medical Research Foundation) for their skilled assistance and contributions on this project. SEE was supported by Nutrition Science, Hawthorne, Fields-Rohlfing and Charley Fellowships. HDS was supported by Maksud Fellowship in Exercise Physiology. MMR was supported by K01DK103829 from the National Institutes of Health. SAN was supported by KL2TR002370 as part of the Oregon Clinical & Translational Research Institute Clinical Translational Science Award UL1TR002371 from the National Institutes of Health.

Funding information

HHS | National Institutes of Health (NIH),Grant/Award Number: K01DK103829 and KL2TR002370

Abbreviations:

ATG6	autophagy-related protein 6 (Beclin-1)
ATG7	autophagy-related protein 7
BNIP3	Bcl-2/adenovirus E1B interacting protein 3
CI	ETS complex I
CII	ETS complex II
CIII	ETS complex III

CIV	ETS complex IV
CV	ETS complex V
E	uncoupled respiration
ETF	electron transfer flavoprotein
ETS	electron transport system
HADH	hydroxyacyl-coenzyme A dehydrogenase
IMFM	intermyofibrillar mitochondria
L	leak respiration
LC3	microtubule-associated protein 1A/1B light chain 3A
MYO	myofibrillar
P	oxidative phosphorylation
SSM	subsarcolemmal mitochondria

REFERENCES

1. Fischer F, Hamann A, Osiewacz HD. Mitochondrial quality control: an integrated network of pathways. Trends Biochem Sci. 2012;37:284–292. [PubMed: 22410198]
2. Møller AB, Kampmann U, Hedegaard J, et al. Altered gene expression and repressed markers of autophagy in skeletal muscle of insulin resistant patients with type 2 diabetes. Nat Publ Group. 2017;7:1–11.
3. Nilsson MI, Dobson JP, Greene NP, et al. Abnormal protein turnover and anabolic resistance to exercise in sarcopenic obesity. FASEB J. 2013;27:3905–3916. [PubMed: 23804240]
4. Gonzalez CD, Lee M-S, Marchetti P, et al. The emerging role of autophagy in the pathophysiology of diabetes mellitus. Autophagy. 2011;7:2–11. [PubMed: 20935516]
5. Koga H, Kaushik S, Cuervo AM. Protein homeostasis and aging: the importance of exquisite quality control. Ageing Res Rev. 2011;10:205–215. [PubMed: 20152936]
6. Hamilton KL, Miller BF. Mitochondrial proteostasis as a shared characteristic of slowed aging: the importance of considering cell proliferation. J Physiol. 2017;595:6401–6407. [PubMed: 28719097]
7. Gonzalez-Freire M, de Cabo R, Bernier M, et al. Reconsidering the role of mitochondria in aging. GERONA. 2015;70:1334–1342.
8. Pinti MV, Fink GK, Hathaway QA, Durr AJ, Kunovac A, Hollander JM. Mitochondrial dysfunction in type 2 diabetes mellitus: an organ-based analysis. Am J Physiol Endocrinol Metab. 2019;316:E268–E285. [PubMed: 30601700]
9. Davies KJ, Packer L, Brooks GA. Biochemical adaptation of mitochondria, muscle, and whole-animal respiration to endurance training. Arch Biochem Biophys. 1981;209:539–554. [PubMed: 7294809]
10. Robinson MM, Dasari S, Konopka AR, et al. Enhanced protein translation underlies improved metabolic and physical adaptations to different exercise training modes in young and old humans. Cell Metab. 2017;25:581–592. [PubMed: 28273480]
11. Bujak AL, Crane JD, Lally JS, et al. AMPK activation of muscle autophagy prevents fasting-induced hypoglycemia and myopathy during aging. Cell Metab. 2015;21:883–890. [PubMed: 26039451]
12. Fu T, Xu Z, Liu L, et al. Mitophagy directs muscle-adipose crosstalk to alleviate dietary obesity. Cell Rep. 2018;23:1357–1372. [PubMed: 29719250]

13. Ju J-S, Jeon S-I, Park J-Y, et al. Autophagy plays a role in skeletal muscle mitochondrial biogenesis in an endurance exercise-trained condition. J Physiol Sci. 2016;66:417–430. [PubMed: 26943341]
14. Lira VA, Okutsu M, Zhang M, et al. Autophagy is required for exercise training-induced skeletal muscle adaptation and improvement of physical performance. FASEB J. 2013;27:4184–4193. [PubMed: 23825228]
15. Yan Z, Kronemberger A, Blomme J, et al. Exercise leads to unfavourable cardiac remodelling and enhanced metabolic homeostasis in obese mice with cardiac and skeletal muscle autophagy deficiency. Sci Rep. 2017;7:1143–7894. [PubMed: 28442766]
16. Chen CCW, Erlich AT, Hood DA. Role of Parkin and endurance training on mitochondrial turnover in skeletal muscle. Skelet Muscle. 2018;8:1–14. [PubMed: 29304851]
17. He C, Bassik MC, Moresi V, et al. Exercise-induced BCL2-regulated autophagy is required for muscle glucose homeostasis. Nature. 2012;481:511–515. [PubMed: 22258505]
18. Konopka AR, Asante A, Lanza IR, et al. Defects in mitochondrial efficiency and H2O2 emissions in obese women are restored to a lean phenotype with aerobic exercise training. Diabetes. 2015;64:2104–2115. [PubMed: 25605809]
19. Laker RC, Drake JC, Wilson RJ, et al. Ampk phosphorylation of Ulk1 is required for targeting of mitochondria to lysosomes in exercise-induced mitophagy. Nat Commun. 2017;8:548. [PubMed: 28916822]
20. Ehrlicher SE, Stierwalt HD, Newsom SA, Robinson MM. Skeletal muscle autophagy remains responsive to hyperinsulinemia and hyperglycemia at higher plasma insulin concentrations in insulin-resistant mice. Physiol Rep. 2018;6:e13810–e13813. [PubMed: 30047243]
21. Fritzen AM, Frøsig C, Jeppesen J, et al. Role of AMPK in regulation of LC3 lipidation as a marker of autophagy in skeletal muscle. Cell Signal. 2016;28:663–674. [PubMed: 26976209]
22. Newsom SA, Miller BF, Hamilton KL, Ehrlicher SE, Stierwalt HD, Robinson MM. Long-term rates of mitochondrial protein synthesis are increased in mouse skeletal muscle with high-fat feeding regardless of insulin-sensitizing treatment. Am J Physiol Endocrinol Metab. 2017;313:E552–E562. [PubMed: 28698283]
23. Lark DS, Kwan JR, McClatchey PM, et al. Reduced nonexercise activity attenuates negative energy balance in mice engaged in voluntary exercise. Diabetes. 2018;67:831–840. [PubMed: 29511026]
24. Miller BF, Robinson MM, Bruss MD, Hellerstein M, Hamilton KL. A comprehensive assessment of mitochondrial protein synthesis and cellular proliferation with age and caloric restriction. Aging Cell. 2011;11:150–161. [PubMed: 22081942]
25. Ritov VB, Menshikova EV, He J, Ferrell RE, Goodpaster BH, Kelley DE. Deficiency of subsarcolemmal mitochondria in obesity and Type 2 diabetes. Diabetes. 2004;54:8–14.
26. Busch R, Kim Y, Neese RA, et al. Measurement of protein turnover rates by heavy water labeling of nonessential amino acids. Biochim Biophys Acta. 2006;1760:730–744. [PubMed: 16567052]
27. Lanza IR, Nair KS. Functional assessment of isolated mitochondria in vitro. Meth. Enzymol. 2009;457:349–372.
28. Dasari S, Newsom SA, Ehrlicher SE, Stierwalt HD, Robinson MM. Remodeling of skeletal muscle mitochondrial proteome with high-fat diet involves greater changes to beta-oxidation than electron transfer proteins in mice. Am J Physiol Endocrinol Metab. 2018;315:E425–E434. [PubMed: 29812987]
29. Masiero E, Agatea L, Mammucari C, et al. Autophagy is required to maintain muscle mass. Cell Metab. 2009;10:507–515. [PubMed: 19945408]
30. Kim KH, Jeong YT, Oh H, et al. Autophagy deficiency leads to protection from obesity and insulin resistance by inducing Fgf21 as a mitokine. Nat Med. 2012;19:83–92. [PubMed: 23202295]
31. Mizushima N, Yoshimori T. How to interpret LC3 immunoblotting. Autophagy. 2007;3:542–545. [PubMed: 17611390]
32. He C, Levine B. The Beclin 1 interactome. Curr Opin Cell Biol. 2010;22:140–149. [PubMed: 20097051]

33. Turner N, Bruce CR, Beale SM, et al. Excess lipid availability increases mitochondrial fatty acid oxidative capacity in muscle: evidence against a role for reduced fatty acid oxidation in lipid-induced insulin resistance in rodents. Diabetes. 2007;56:2085–2092. [PubMed: 17519422]
34. Nilsson MI, Greene NP, Dobson JP, et al. Insulin resistance syndrome blunts the mitochondrial anabolic response following resistance exercise. Am J Physiol Endocrinol Metab. 2010;299:E466–E474. [PubMed: 20606077]
35. Anderson EJ, Lustig ME, Boyle KE, et al. Mitochondrial H2O2 emission and cellular redox state link excess fat intake to insulin resistance in both rodents and humans. J Clin Invest. 2009;119:573–581. [PubMed: 19188683]
36. Wang Y, Nartiss Y, Steipe B, McQuibban GA, Kim PK. ROS-induced mitochondrial depolarization initiates PARK2/PARKIN-dependent mitochondrial degradation by autophagy. Autophagy. 2014;8:1462–1476.
37. Novak I, Kirkin V, McEwan DG, et al. Nix is a selective autophagy receptor for mitochondrial clearance. EMBO Rep. 2010;11:45–51. [PubMed: 20010802]
38. Vainshtein A, Tryon LD, Pauly M, Hood DA. Role of PGC-1α during acute exercise-induced autophagy and mitophagy in skeletal muscle. Am J Physiol Cell Physiol. 2015;308:C710–C719. [PubMed: 25673772]
39. Drake JC, Wilson RJ, Yan Z. Molecular mechanisms for mitochondrial adaptation to exercise training in skeletal muscle. FASEB J. 2016;30:13–22. [PubMed: 26370848]
40. Vainshtein A, Hood DA. The regulation of autophagy during exercise in skeletal muscle. J Appl Physiol. 2016;120:664–673. [PubMed: 26679612]
41. Rosa-Caldwell ME, Brown JL, Lee DE, et al. Autophagy activation, not peroxisome proliferator-activated receptor γ coactivator 1α, may mediate exercise-induced improvements in glucose handling during diet-induced obesity. Exp Physiol. 2017;102:1194–1207. [PubMed: 28639297]
42. Lo Verso F, Carnio S, Vainshtein A, Sandri M. Autophagy is not required to sustain exercise and PRKAA1/AMPK activity but is important to prevent mitochondrial damage during physical activity. Autophagy. 2014;10:1883–1894. [PubMed: 25483961]
43. Holloszy JO. Biochemical adaptations in muscle. Effects of exercise on mitochondrial oxygen uptake and respiratory enzyme activity in skeletal muscle. J Biol Chem. 1967;242:2278–2282. [PubMed: 4290225]
44. Garcia-Roves P, Huss JM, Han D-H, et al. Raising plasma fatty acid concentration induces increased biogenesis of mitochondria in skeletal muscle. Proc Natl Acad Sci U S A. 2007;104:10709–10713. [PubMed: 17548828]
45. Koves TR, Noland RC, Bates AL, Henes ST, Muoio DM, Cortright RN. Subsarcolemmal and intermyofibrillar mitochondria play distinct roles in regulating skeletal muscle fatty acid metabolism. Am J Physiol Cell Physiol. 2005;288:C1074–C1082. [PubMed: 15647392]
46. Lanza IR, Zabielski P, Klaus KA, et al. Chronic caloric restriction preserves mitochondrial function in senescence without increasing mitochondrial biogenesis. Cell Metab. 2012;16:777–788. [PubMed: 23217257]
47. Duran A, Amanchy R, Linares JF, et al. p62 is a key regulator of nutrient sensing in the mTORC1 pathway. Mol Cell. 2011;44:134–146. [PubMed: 21981924]
48. Koves TR, Ussher JR, Noland RC, et al. Mitochondrial overload and incomplete fatty acid oxidation contribute to skeletal muscle insulin resistance. Cell Metab. 2008;7:45–56. [PubMed: 18177724]
49. Nabben M, Hoeks J, Moonen-Kornips E, et al. Significance of uncoupling protein 3 in mitochondrial function upon mid- and long-term dietary high-fat exposure. FEBS Lett. 2011;585:4010–4017. [PubMed: 22115550]
50. Boudina S, Sena S, Sloan C, et al. Early mitochondrial adaptations in skeletal muscle to diet-induced obesity are strain dependent and determine oxidative stress and energy expenditure but not insulin sensitivity. Endocrinology. 2012;153:2677–2688. [PubMed: 22510273]
51. Hancock CR, Han D-H, Chen M, et al. High-fat diets cause insulin resistance despite an increase in muscle mitochondria. Proc Natl Acad Sci USA. 2008;105:7815–7820. [PubMed: 18509063]

52. Seifert EL, Estey C, Xuan JY, Harper M-E. Electron transport chain-dependent and -independent mechanisms of mitochondrial H2O2 emission during long-chain fatty acid oxidation. J Biol Chem. 2010;285:5748–5758. [PubMed: 20032466]

53. Shimazu T, Furuse T, Balan S, et al. Role of METTL20 in regulating β-oxidation and heat production in mice under fasting or ketogenic conditions. Sci Rep. 2018;8:1179–1179. [PubMed: 29352221]

54. Jaleel A, Short KR, Asmann YW, et al. In vivo measurement of synthesis rate of individual skeletal muscle mitochondrial proteins. Am J Physiol Endocrinol Metab. 2008;295:E1255–E1268. [PubMed: 18765679]

55. Miller BF, Wolff CA, Peelor FF III, Shipman PD, Hamilton KL. Modeling the contribution of individual proteins to mixed skeletal muscle protein synthetic rates over increasing periods of label incorporation. J Appl Physiol. 2015;118:655–661. [PubMed: 25593288]

56. Picard M, Taivassalo T, Ritchie D, et al. Mitochondrial structure and function are disrupted by standard isolation methods. PLoS One. 2011;6:e18317-e18317.

57. Twig G, Elorza A, Molina AJA, et al. Fission and selective fusion govern mitochondrial segregation and elimination by autophagy. EMBO J. 2008;27:433–446. [PubMed: 18200046]

58. Antoun G, McMurray F, Thrush AB, et al. Impaired mitochondrial oxidative phosphorylation and supercomplex assembly in rectus abdominis muscle of diabetic obese individuals. Diabetologia. 2015;58:2861–2866. [PubMed: 26404066]

59. Lundsgaard A-M, Holm JB, Sjøberg KA, et al. Mechanisms preserving insulin action during high dietary fat intake. Cell Metab. 2019;29:50–63.e54. [PubMed: 30269983]

60. Lai N, Kummitha C, Hoppel C. Defects in skeletal muscle subsarcolemmal mitochondria in a non-obese model of type 2 diabetes mellitus. PLoS One. 2017;12:e0183978.

61. Cardinale DA, Larsen FJ, Schiffer TA, et al. Superior intrinsic mitochondrial respiration in women than in men. Front Physiol. 2018;9:1133. [PubMed: 30174617]

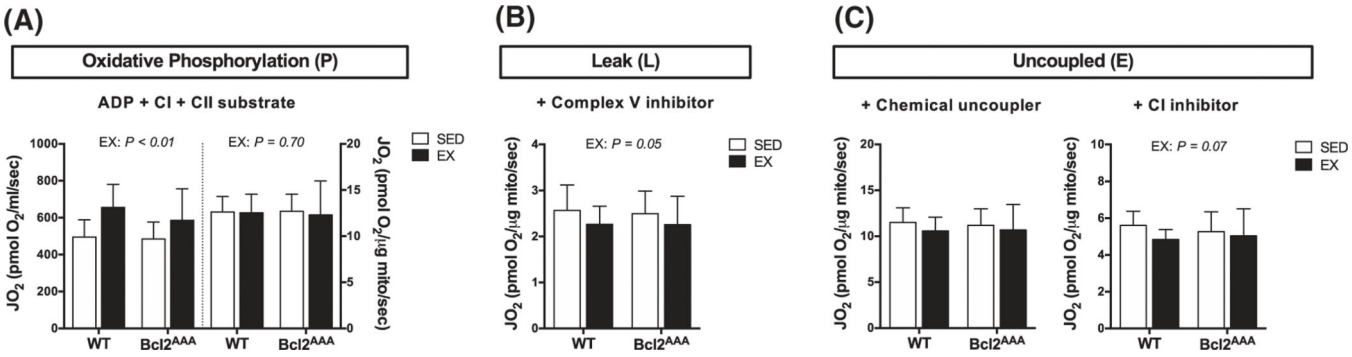

FIGURE 1.

Bcl2-mediated autophagy is not required for mitochondrial respiratory adaptations to exercise training. Mitochondrial respiration of isolated mitochondria from quadriceps muscle of wild-type and Bcl2^{AAA} mice that performed 8 wk of exercise training (EX) or remained sedentary (SED). A, Complex I (CI) and complex II (CII) substrate-linked oxygen consumption (JO_2) during oxidative phosphorylation (P) with nonlimiting ADP. Rates of JO_2 are expressed as absolute units (pmol O_2/mL/sec; left) and relative to protein content (pmol O_2/μg protein/sec; right). B, CI and CII substrate-linked oxygen consumption (JO_2) during leak (L) respiration after the addition of oligomycin, a complex V inhibitor. Rates of JO_2 are expressed as relative units (pmol O_2/μg protein/sec). C, CI and CII substrate-linked oxygen consumption (JO_2) during uncoupled electron transfer system (E) respiration after the addition of the chemical uncoupler, FCCP (left) and after the addition of rotenone, a CI inhibitor (right). Rates of JO_2 are expressed as relative units (pmol O_2/μg protein/sec). Data are means ± SD; n = 12–17. Two-way ANOVAs were used to test for effects of exercise and genotype. *P* values are main effects

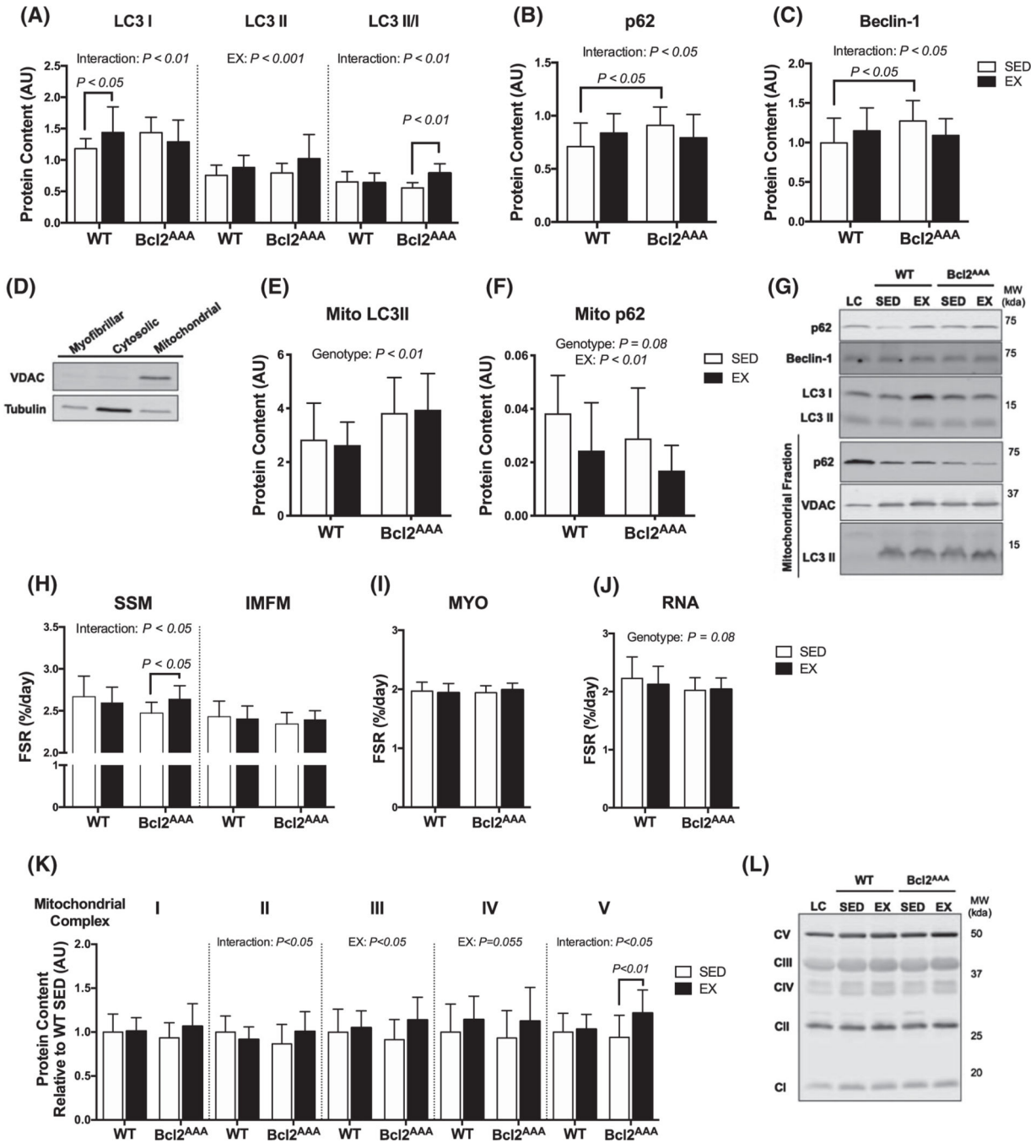

FIGURE 2.

Greater protein turnover contributes to mitochondrial adaptations in autophagy-deficient mice. Quadricep and gastrocnemius muscles were collected after a 4-h fast and 36 h after exercise from wild-type and Bcl2^{AAA} mice that performed 8 wk of exercise training (EX) or remained sedentary (SED). Whole tissue lysates were prepped from quadriceps and mitochondria were isolated from gastrocnemius muscle for immunoblotting. A, Protein content of the autophagy markers LC3I, LC3II, and the ratio of LC3 II/I, B, p62 and (C) Beclin-1 measured with immunoblotting expressed as arbitrary units. D, Demonstration of

VDAC and tubulin content in the skeletal muscle fractions. E, Protein content in the mitochondrial fraction of the autophagy markers LC3II and (F) p62 normalized to VDAC content and expressed as arbitrary units. G, Representative blots for (A-F) with loading controls (LC). H, Fractional synthesis rates (%/day) of proteins in the subsarcolemmal (SSM) and intermyofibrillar (IMFM) mitochondrial fractions of quadriceps muscle during 14 d of deuterium oxide labeling. I, Fractional synthesis rates (%/day) of the myofibrillar (MYO) fraction of quadriceps muscle. J, Fractional synthesis rates (%/day) of RNA extracted from quadriceps muscle. K, Protein content of subunits in mitochondrial respiratory complexes I-V measured with immunoblotting expressed in arbitrary units relative to WT SED values. L, Representative blots for (K) with loading control (LC). Full blot images and Ponceau stain of membranes are in supplemental data. Data are mean ± SD. Two-way ANOVA tested effects of exercise and genotype. *P* values are main effects or post hoc comparisons when significant interaction effects were observed. Protein content data are n = 12–17, FSR data are n = 12–16

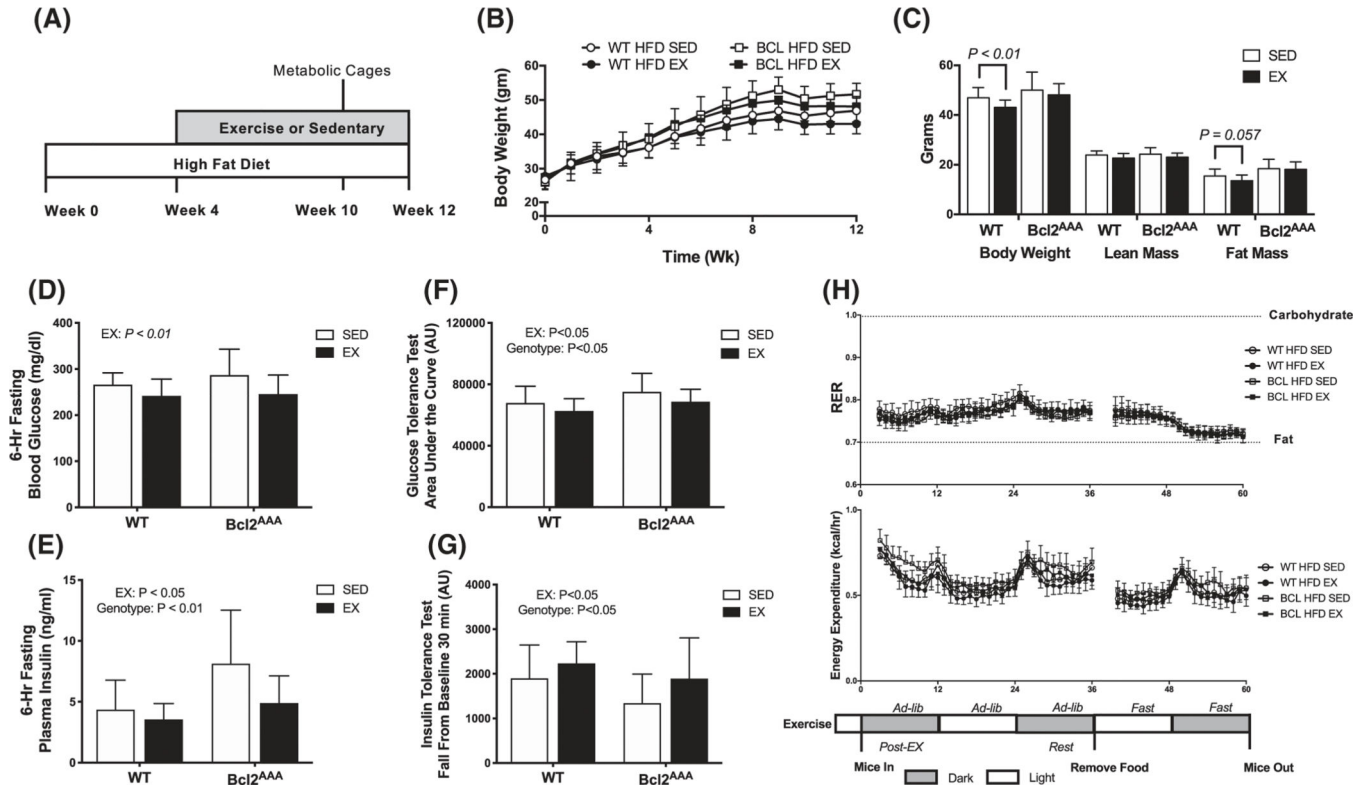

FIGURE 3.

Whole-body metabolic phenotype following high-fat feeding and exercise training. A, Wild-type and Bcl2^{AAA} mice consumed a high-fat diet (HFD, 60% kcal from fat) for 4 wk then performed 8 wk of exercise training (EX) or remained sedentary (SED). During week 10, mice were individually housed in metabolic cages for 3 d. B, Body weight (grams) measured weekly. C, Body weight (grams) measured at 10 wk with lean and fat mass (grams), obtained from DEXA. D, Glucose concentrations (mg/dL) measured with a handheld glucometer in blood collected from a tail vein after a 6-h fast. E, Plasma insulin concentrations (ng/mL) measured with a commercial ELISA kit in blood collected from a tail vein after a 6-h fast. F, Area under the curve for a 2-h glucose tolerance test. Mice were fasted for 6 h then glucose was provided with an intraperitoneal injection of 2 g/kg body wt of a 20% dextrose solution. G, Fall from baseline in the first 30 min of a 2-h insulin tolerance test. Mice were fasted for 4 h then insulin injected intraperitoneally at 0.5 IU/kg body wt. H, Respiratory exchange ratio (RER; top) and energy expenditure (kcal/hr; bottom) calculated as 1-h averages from indirect calorimetry immediately post-exercise, in a rested state, and in a fasted state. Data are mean ± SD. Data in panel (C) were analyzed by Student's *t*-test. Two-way ANOVA tested for effects of genotype and exercise in all other panels and *P* values are main effects. Group sizes are n = 12–17

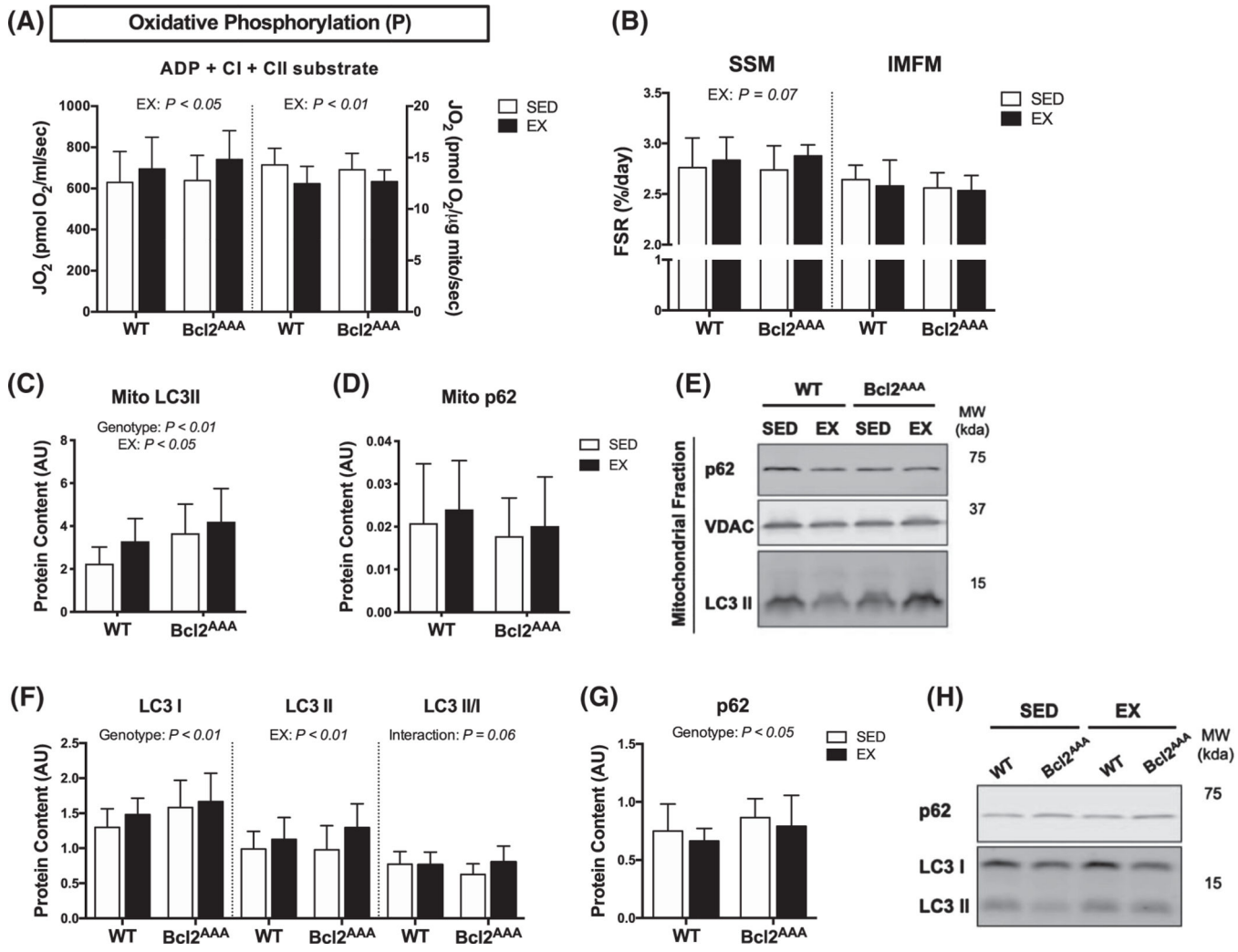

FIGURE 4.

High-fat feeding did not impair mitochondrial adaptations to exercise training. Quadricep and gastrocnemius muscles were collected after a 4-h fast and 36 h after exercise from wild-type and Bcl2^{AAA} mice given a 60% high-fat diet for 12 wk and performed 8 wk of exercise training (EX) or remained sedentary (SED). A, Respiration of isolated mitochondria. Complex I (CI) and complex II (CII) substrate-linked oxygen consumption (JO_2) during oxidative phosphorylation (P) with non-limiting ADP. Rates of JO_2 are expressed as absolute units (pmol O_2/ml/sec; left) and relative to protein content (pmol O_2/µg protein/sec; right). B, Fractional synthesis rates (%/day) of proteins in the subsarcolemmal (SSM) and intermyofibrillar (IMFM) mitochondrial fractions of quadriceps muscle. C, Protein content in the gastrocnemius mitochondrial fraction of the autophagy markers LC3II and (D) p62 normalized to VDAC content and expressed as arbitrary units. E, Representative blots for (C and D). F, Protein content of the autophagy markers LC3I, LC3II, and the ratio of LC3 II/I and G, p62 measured in quadriceps with immunoblotting expressed as arbitrary units. H, Representative blots for (F & G). Full blot images and Ponceau stain of membranes are in supplemental data. Data are mean ± SD. Two-way ANOVA tested for effects of genotype and exercise. *P* values are main effects. Group sizes are n = 12–17

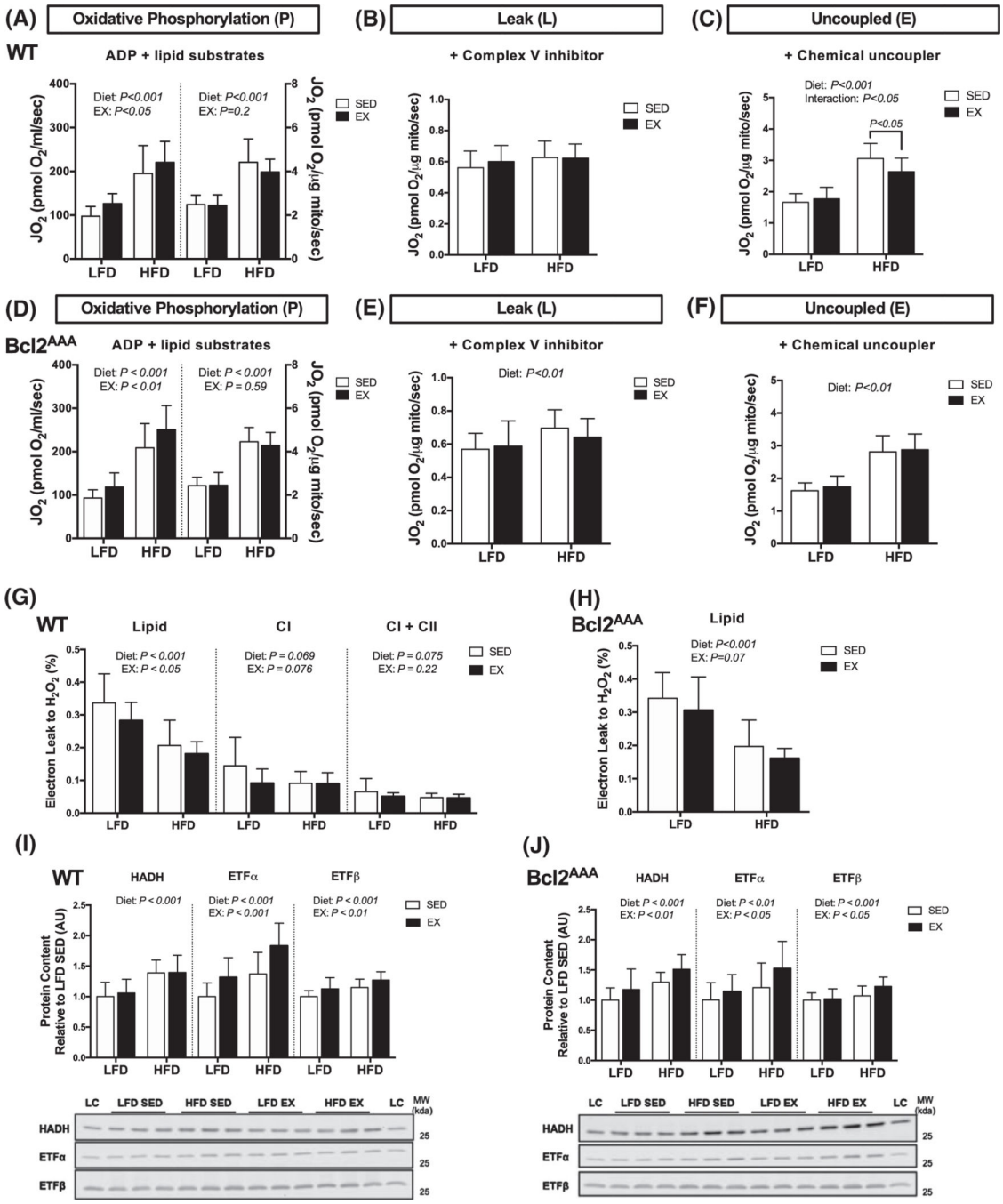

FIGURE 5.

Independent effects of exercise and high-fat feeding to induce mitochondrial lipid oxidation adaptations. Quadricep muscles were collected after a 4-h fast and 36 h after exercise from wild-type and Bcl2^{AAA} mice given a low-fat (LFD) or 60% high-fat diet (HFD) for 12 wk and performed 8 wk of exercise training (EX) or remained sedentary (SED). A and D, Respiration of isolated mitochondria. Lipid substrate-linked oxygen consumption (JO_2) during oxidative phosphorylation (P) with non-limiting ADP. Rates of JO_2 are expressed as absolute units (pmol O_2/sec; left) and relative to protein content (pmol O_2/µg protein/sec;

right). B and E, Lipid substrate-linked oxygen consumption (JO_2) during leak (L) respiration after the addition of oligomycin, a complex V inhibitor. Rates of JO_2 are expressed as relative units (pmol O_2/μg protein/sec). C and F, Lipid substrate-linked oxygen consumption (JO_2) during uncoupled electron transfer system (E) respiration after the addition of the chemical uncoupler, FCCP. Rates of JO_2 are expressed as relative units (pmol O_2/μg protein/sec). G and H, Electron leak to H_2O_2 calculated from H_2O_2 emission during oxidative phosphorylation and expressed as a percentage of oxygen consumption. I and J, Protein content of HADH, ETF subunits α and β, expressed as arbitrary units relative to LFD SED values with representative blot images. Full blot images and Ponceau stain of membranes are in supplemental data. Data are means ± SD. Two-way ANOVA tested for effects of diet and exercise. *P* values are main effects or post-hoc comparisons when significant interactions effects were observed. Group sizes are n = 12–17, except panels (C and F) n = 11–13

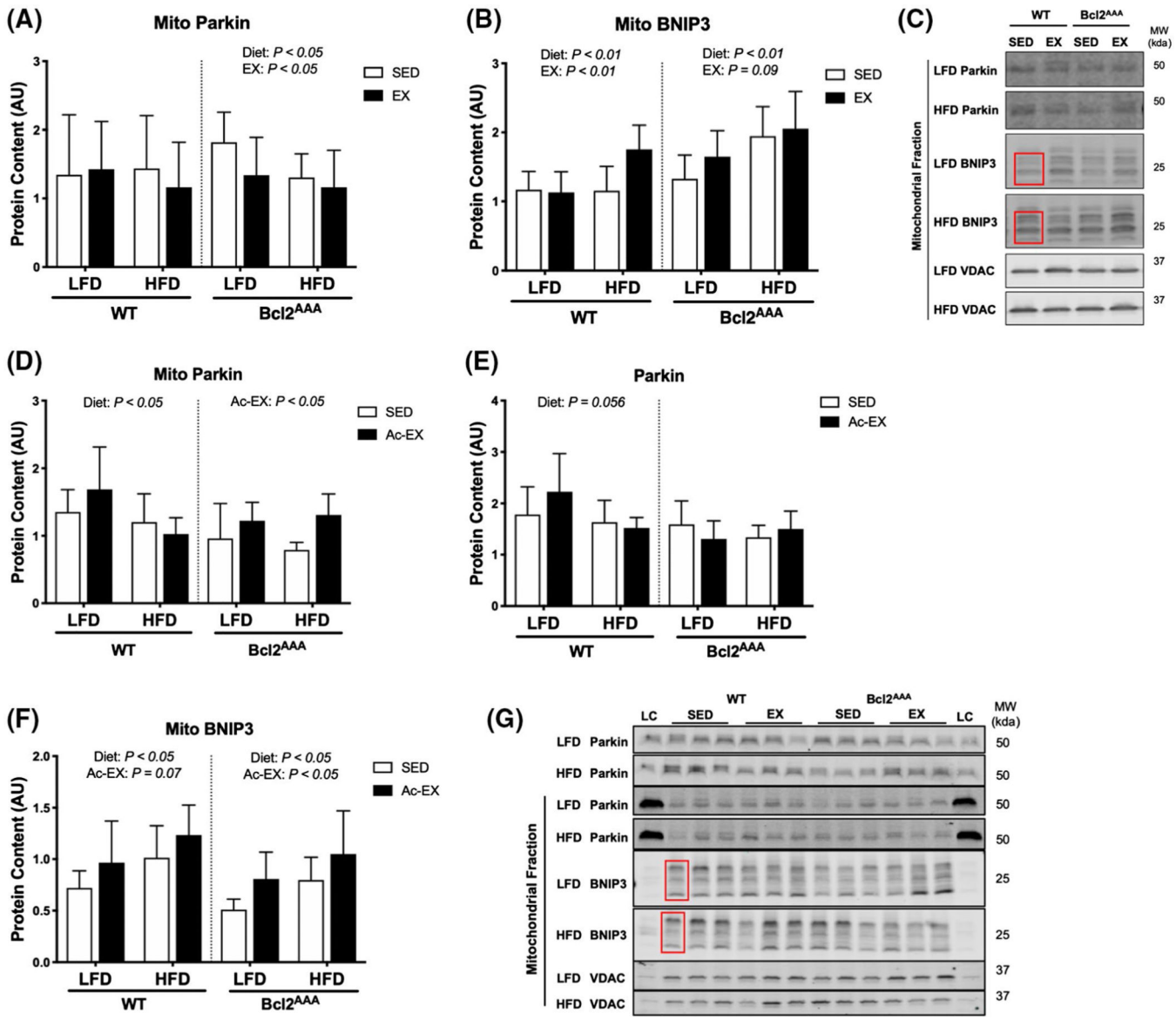

FIGURE 6.

Exercise training and acute exercise upregulate parallel autophagy pathways during high-fat feeding. Gastrocnemius muscles were collected after a 4-h fast and 36 h after exercise from wild-type and Bcl2^{AAA} mice given a 60% high-fat diet for 12 wk and performed 8 wk of exercise training (EX) or remained sedentary (SED). A separate group of wild-type and Bcl2^{AAA} mice given a low-fat (LFD) or high-fat diet (HFD) for 12 wk then performed a single bout of treadmill exercise (Ac-EX) or remained sedentary (SED). Mitochondria were isolated from gastrocnemius muscle for immunoblotting. A, Parkin content and (B) BNIP3 content in the mitochondrial fraction of exercise trained mice normalized to VDAC content and expressed as arbitrary units (AU). C, Representative blots for (A and B). D, Parkin content in the mitochondrial fraction normalized to VDAC as a loading control and expressed as AU. E, Parkin content in the whole cell lysate expressed as AU. F, BNIP3 in the mitochondrial fraction normalized to VDAC as a loading control and expressed as AU.

BNIP3 consistently appeared as triplicate bands, therefore all three bands specified by the red box were quantified. G, Representative blot images for (D-F). Full blot images and Ponceau stain of membranes are in supplemental data. Data are means ± SD. Two-way ANOVA tested for effects of diet and exercise within each genotype. *P* values are main effects. Group sizes are n = 12–17 for exercise trained mice and n = 5–6 for acute exercise mice